Hydrologic Secular Trends and Variations of the Eurasian and North American Permafrost Watersheds from GRACE, SSM/I and AMSR-E Observations

EGU2009-3212 Reginald R. Muskett & Vladimir E. Romanovsky Geophysical Institute, University of Alaska Fairbanks, USA, reginald.muskett@gmail.com EGU2009-3212

ABSTRACT

The northern hemisphere permafrost regions compose the largest component by area of the cryosphere. Over the last century, substantial changes in storage and cycling of fresh water have been observed. Observations of the globally distributed hydrologic mass change from the Gravity Recovery and Climate Experiment (GRACE) mission offer to provide a greater understanding of the processes controlling redistribution of water mass. Using nominal monthly GRACE grids, complete to degree and order 40 (which act as a low-pass spatial-temporal filter) adjusted for post-glacial rebound we investigate the hydrologic mass change of the Eurasian and North American watershed regions. The extent of continuous permafrost in the watersheds in Eurasia varies from the Ob' which has the least to the Lena (includes part of the Yedoma Ice Complex) which has the largest. The Ob' watershed contains the least extent of continuous permafrost in this study. GRACE-derived watershed region-average time series show strongly positive secular trends and seasonal variations. Watershed region-averaged time series were derived from the Special Scanning Microwave/Imager (SSM/I) and the Advanced Microwave Scanning Radiometer-for the Earth Observation System (AMSR-E) for snow water equivalent, soil moisture and vegetation water content respectively. The seasonal maxima and minima derived from SSM/I and AMSR-E occur one-to-two months ahead of those of GRACE. Secular trends of snow water equivalent, soil moisture and vegetation water content had neither significant gain nor loss over the time period. Partitioning the watershed regions into 5° by 5° sub-regions, showed GRACE sub-region secular trends varied from south-to-north and west-to-east, suggesting variation at the source of water equivalent mass change. SSM/I and AMSR-E sub-region secular trends showed no significant gains or losses of water (snow, soil moisture or vegetation content); however, mean water contents vary across sub-regions of each watershed. The Eurasian watersheds GRACE-derived water equivalent mass gains were 22.69 ± 13.49 km^3/yr for the Ob', 37.75 ± 8.83 km^3/yr for the Yenisei and 44.69 ± 8.36 km^3/yr for the Lena from August 2002 through March 2008. The Mackenzie watershed had a GRACE-derived water equivalent mass loss of 5.58 ± 7.18 km^3/yr (not significant) in the same time period. Therefore, the source of the GRACE 40 by 40 degree and order secular trends and variations of water equivalent mass changes must be occurring beneath the land surface and soil layer of the Eurasian and North American permafrost watershed regions.

Introduction

Two factors which act as primary controls on hydrologic processes in the northern latitude regions are the presence or absence of permafrost and the thickness of the active-layer (the top layer of soil that thaws during the summer and freezes in autumn) (White et al., 2007). Geographically diverse observations of permafrost temperature (~ 2m depth) show temporally and spatially non-uniform changes, mostly increases, over the twentieth century (Osterkamp, 2007; Romanovsky et al., 2007). These correlate well to surface air temperature changes on decadal time scales. Permafrost temperatures in eastern Siberia show the largest magnitude of increases of a few degrees centigrade whereas parts of western North America shows lower magnitudes of permafrost temperature increases. Increasing surface air temperatures, from climate warming over the same period cannot fully account for increasing permafrost temperatures, suggesting that variability and secular trends in snow cover may be a contributing factor. Satellite data suggest that the continuous permafrost zone in Siberia had increases in lake area (thermokarst lakes formed by processes of degradation of permafrost) of up to 12%, and the number of lakes increased by 4% over the last 30 years.

Global satellite observations from the Gravity Recovery and Climate Experiment (GRACE) have shown to be great promise in detecting secular trends and spatial-temporal variations in land and ocean hydrologic mass changes since the operational period beginning in August 2002 and ongoing (Frappart et al., 2006; Niu et al., 2007; Syed et al., 2007; Ramillien et al., 2008). We investigate the GRACE observations for addressing permafrost and active layer change in the Lena and Ob' River watershed regions in Eurasia and the Mackenzie River watershed region in North America (Fig. 1).

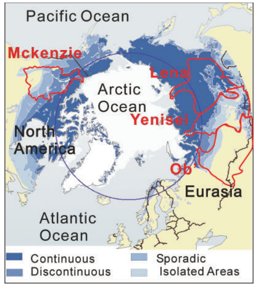

Figure 1. Northern Hemisphere Permafrost regions and watersheds. (Background map from the UN Environmental Program, Arctic Environment Atlas.)

GRACE Water Equivalent Mass Change

The co-orbiting satellites of GRACE do not measure variations in gravity or mass directly (Chambers, 2006). Rather, measurements in the variations of the inter-satellite range (range rate and range acceleration) is measured, coupled with accurate GPS location relative to the International Terrestrial Reference Frame 2005, to estimate values of the time change in spherical harmonic geopotential coeficients, ΔC and ΔS, to degree and order 40. Level-3 Release-04 coefficients are computed from Level-2 coefficients, up to degree and order 60, after time-mean reduction and de-striping. These are then used in the expansion below to estimate changes of water mass:

$$\Delta h(\phi,\lambda,t) = \frac{a_e \rho_e}{3\rho_w} \sum_{l=0}^{40} \sum_{m=0}^{l} \frac{(2l+1)}{(1+k_l)} W_l P_{lm} \sin\phi \left[\Delta C_{lm}(t)\cos m\lambda + \Delta S_{lm}(t)\sin m\lambda\right]$$

$$W_l = \exp\left[\frac{(lr/a_e)^2}{4\ln(2)}\right]$$

P_{lm} : Normalized Legendre polynomials
$\Delta C_{lm}, \Delta S_{lm}$: Normalized time-varying Stokes spherical harmonic Geopotential coeficients

a_e -- Earth mean radius
ρ_e -- Earth mean density
ρ_w -- Density of water
r -- Spatial radius
t -- Time
ϕ, λ -- Latitude and longitude
k_l -- Love numbers

Processing of the nominal monthly global grids includes adjustments for removal of the atmospheric mass changes, ocean (fluid) and land (solid) tides and pole-tides, and the longer-term mean field (GRACE-derived geoid). Mass changes are therefore in the radial coordinate, relative to the satellite-pair common center of mass and the Earth's center of mass. Mass changes on ocean basins and the terrestrial watersheds, not associated with vertical loading/unloading of mass are by way mass transters, i.e. flows tangential to the geoid.

GRACE Release 4 Level-3 300 km smoothing kernal land and ocean monthly grids, from August 2002 through March 2008, were combined to give global coverage, then adjusted by a Glacial Isostatic Adjustment grid (Paulson et al., 2007). Figure 2. Shows the GRACE water equivalent thickness changes on the terrestrial portion of the northern hemisphere at Septermber 2006, and May 2007. These were chosen to illustrate the spatial distribution on terrestrial sourced regions. The GRACE mass change minimum occurs in September and maximum in May.

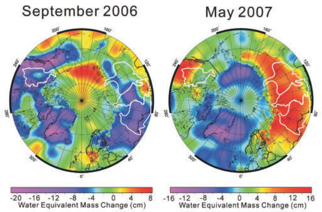

Figure 2. Terrestrial northern hemisphere GRACE water equivalent mass changes (cm) during September 2006 and May 2007.

Vegetation and Soil Water Contents

Global vegetation water content (VWC) and soil moisture content (SMC) were derived from the AMSR-E sensor and provided by NSIDC. Vegetation water content and soil moisture estimates in units of kg/m^2 and g/cm^3, respectively, were derived using the normalized polarization difference algorithm employing the C and X channels from global orbit swaths acquired daily (*Njoku et al.*, 2003; *Njoku and Chan*, 2006). Nominal spatial resolution is about 38 square kilometers at 10.7 GHz. Data were gridded in the equal-area Ease-grid projection system at 25-by-25 kilometer grid intervals. Vegetation water content derives from the leaf structure of canopy and vesicular plants on the ground. Soil moisture retrieval derives from a one centimeter thick layer.

During winter months, December through March, fractional retrievals of vegetation water and soil moisture were spatially correlated with large ice-covered lakes, groups of ice-covered lakes, and northern coastal areas. Skin temperatures derived from the Moderate Resolution Imaging Spectroradiometer (MODIS) indicated frozen ground conditions. We interpret these very-low winter retrievals to be errors of the sensor and polarization algorithm. Winter retrievals were removed from the time series.

Snow Water Equivalent

Global snow water equivalent estimates on a monthly time basis derive from the NOAA Defense Meteorological Satellite Program by the Special Sensor Micro-wave/Imagers (SSM/I), are proveded by the National Snow and Ice Data Center (http://nsidc.org/data/docs/dac/nsidc_0271_ease_grid_swe_climatology.gd.html). SSMI and its predecessor instrument, has been retrieving passive microwave data since 1978. Snow Water Equivalent (SWE) estimates in units of millimeters were derived using the horizontally polarized difference algorithm for the 19 and 37 GHz channels from daily orbit swath acquisitions (Chang et al., 1987). Daily retrievals are averaged to compose monthly estimates. Missing retrievals due to swath coverage gaps are interpolated from neighboring swaths. Sensor resolution is about 69 by 43 square kilometers. The monthly data are gridded in the equal-area Ease-grid projection system at about 25-by-25 kilometer grid intervals.

In-Situ Runoff

Measurements (at gauging stations) of surface water discharge (runoff) in the watersheds were provided by ArcticRIMS (daily/monthly provisional data from 2000 through 2009) and R-Arctic-NET (archive monthly data from 1930 through 2000). Monthly discharge from stations at Kusur (Lena), Igarka (Yenisei), Salekhard (Ob') and Arctic Red River (Mackenzie) were primarily used. The archival periods of the discharged records of each watershed stations used varies in total number of years; Kusur covered a period from 1935 through 2000, Igarka covered a period from 1936 through 1999, Salekhard covered a period from 1930 through 1999, and Arctic Red River covered a period from 1972 through 2000. The archival records were compared to the provisional records to help identify discharge anomalies.

Method

Monthly GRACE water equivalent mass change is compared to AMSR-E VWC and SMC, and SSM/I SWE using the geographic extents of the Lena, Yenisei, Ob' and Mackenzie watersheds. Area-average sample mean, standard deviation and standard error are computed. The monthly area-average means and standard deviations are then plotted in time series. Least-squares trends are computed for each time series. The area of each watershed extent allows for the water equivalent mass changes to be cast as water equivalent volume changes (km^3) which are equivalent to Gigatons of water mass changes.

Results

Figures 3 and 4 show comparisons of area-averaged monthly time series, sample mean and standard deviation, and the least-squares time regressions (GRACE, SSM/I and annual runoff)on the Lena, Yenisei, Ob' and Mackenzie watershed regions.

Seasonal Variations

Over the period from August 2002 through March 2008, secular trends on the watersheds were flat (Fig. 3). Mean vegetation water mass during April-September were 6.17 ± 1.64 Gt (Lena), 7.25 ± 0.86 (Yenisei), 7.39 ± 1.47 Gt (Ob') and 5.28 ± 0.35 Gt (Mackenzie). Mean soil water mass over the same period were 4.30 ± 0.31 Gt (Lena), 4.45 ± 0.46 Gt (Yenisei), 4.49 ± 0.42 Gt (Ob') and 3.79 ± 0.37 Gt (Mackenzie).

On 5°-by-5° sub-regions, latitudinal variations of vegetation water and soil moisture were noted. AMSR-E mean vegetation and soil water mass were lowest on the tundra (0.09 ± 0.06 Gt, 0.23 ± 0.05 Gt Lena delta and lowlands) and higher mean values on boreal forest (0.69 ± 0.09 Gt, 0.39 ± 0.03 Gt Yenisei uplands).

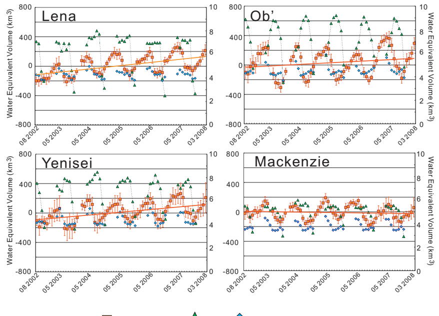

Figure 3. GRACE (■) and AMSR-E (▲ VWC, ◆ SMC) time series. The GRACE secular trends are shown(orange lines) for reference. T-bars indicate standard deviations. Note the differences in scale: -800 to +800 km^3 (GRACE) and 0 to +10 km^3 (AMSR-E).

SSM/I maxima occurred over February through March (Fig.4). The SSM/I maxima occurred ahead of the GRACE maxima by one-to-two months. Monthly runoff showed consistent maxima in June and minima in April. Seasonality of runoff was almost perfectly anti-symmetric to GRACE seasonality. The month of the maximum in mean runoff occurred one-to-two months after the GRACE maxima. The asymmetry of the GRACE time series, gradual increase following the minima corresponds to period of snow mass loading, and the sharp decrease following the maxima corresponds with themonth of maximum runoff of water mass unloading.

Secular Trends

The trends indicate the Lena watershed had the largest water equivalent mass gain of 44.69 ± 8.36 km^3/yr from August 2002 through March 2008 (Fig. 4). The Yenisei watershed had a water equivalent mass gain of 37.75 ± 8.83 km^3/yr. The Ob' had a water equivalent mass gain of 22.69 ± 13.49 km^3/yr. The Mackenzie River watershed in North America had a water equivalent mass change of -5.58 ± 7.18 km^3/yr.

Secular trends in SSM/I SWE were much smaller in magnitude and with larger uncertainties (Fig. 4). The Lena watershed had a gain of 5.88 ± 14.27km^3/yr. The Yenisei and Ob' watersheds showed no change is SWE, -0.02± 9.76 and -0.32 ± 12.42 km^3/yr, respectively. The Mackenzie watershed showed a loss in SWE of 9.94 ± 10.40 km^3/yr.

Secular trends in annual runoff were comparatively stronger on the watersheds, and uncertainties were large (Fig.4). The Lena watershed had a positive annual runoff trend of 39.35 ± 13.30 km^3/yr. The Yenisei watershed had a positive annual runoff trend of 14.64 ± 23.22 km^3/yr. The Ob' watershed had a positive annual runoff trend of 21.71 ± 17.00 km^3/yr. Inspection of August through October 2002 monthly runoff with archival months indicated them to be anomalous. Reports indicate extreme storms in Central Europe in the summer of 2002 caused flooding on major river systems (*Mudelsee et al.*, 2003). We suspect the anomalous-high runoff in summer 2002 in the Ob' was associated with exceptional precipitation. These months were not used in the trend analysis of the Ob'. Interestingly, GRACE water equivalent mass changes on these months in 2002 were also anomalously large in comparison to other years. The secular trend of annual runoff on the Mackenzie watershed was not significant due to the large uncertainty, -0.04 ± 7.76 km^3/yr

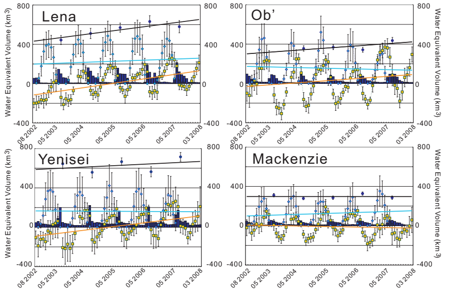

Figure 4. GRACE (■), SSM/I SWE (◆) monthly time series, monthly runoff (▮) and annual runoff time series(●). T-bars indicate standard deviations. Annual runoff is from August through July.

Discussion

In our study, water equivalent mass changes from GRACE solutions up to degree and order 40 which have low noise were presented with surface water changes estimated from space-borne passive microwave sensors on SSM/I and AMSR-E, and in-situ monthly mean runoff in the Arctic permafrost watersheds of the Lena, Yenisei, Ob' and Mackenzie regions. In our preparation of the GRACE grids we used a glacial isostatic adjustment grid ICE-5G (VM2) to remove effects of solid Earth deformation due to post glacial rebound (*Paulson et al.*, 2007). The Lena watershed region contains an appreciable extent and volume of ground ice (Yedoma ice complex) but it and the other watersheds were not glaciated during the Pleistocene, (*Romanovskii et al.*, 2000; *Svendsen et al.*, 2004). Therefore, a solid Earth deformation effect on the area-averaged GRACE monthly water equivalent mass changes and secular trends can be ruled out. In the absence of signal noise and solid Earth deformation, estimates of water mass change by GRACE would be the summation of climate-driven near-surface water mass changes in the radial coodinate relative to the geoid referenced by the ITRF2005 (*Tapley et al.*, 2004). On terrestrial watersheds and ocean basins, the relative mass changes measured in the radial coordinate are due to mass redistributions tangential to the geoid (i.e. mass transfers by *flow*).

Examination of the time series (Fig. 4) indicated that GRACE water equivalent mass changes were sensitive to the timing of mass loading from winter snow water equivalent and mass unloading from spring runoff on the Arctic Eurasian and North American watersheds. Secular trends of water equivalent mass change showed the Lena watershed had the most water mass gain, followed by Yenisei and Ob' (Fig. 4). Secular trends of snow water equivalent from SSM/I were near zero in the Yenisei and Ob' watersheds, and modestly increased in the Lena and Mackenzie watersheds. Annual runoff secular trends showed the largest increase on the Lena, followed by the Ob' and Yenisei, respectively, with the Mackenzie near zero. Qualitatively the annual runoff secular trends agree with trends from 1964 through 2000 (*McCelland et al.*, 2006). For Arctic permafrost watersheds we can formulate a trend-balance relationship as,

$$\Delta T_{GRACE} = \Delta P + \Delta G + \Delta R\,.$$

In this formalism ΔT_{GRACE} is the trend of total change observed by GRACE, ΔP is the trend of effective precipitation change (dominated by snow accumulation minus sublimation and ablation in winter than by wet precipitation minus evapotranpiration in summer), ΔG is the trend of groundwater storage change (neglecting changes in additional surface water impoundments by dams and reservoirs over the short time period), and ΔR is the trend of annual runoff from the watersheds. ΔR captures the mass of winter snow accumulation as mass of spring snow melt.

Figure 5 compares the GRACE, SSM/I and annual runoff secular trend magnitudes and uncertainties in the watersheds. In this perspective the relative agreement of the GRACE with annual runoff secular trends were due to the large uncertainties. The secular trends of snow water equivalent from SSM/I on the Yenisei and Ob' watersheds were near zero, and those on the Lena and Mackenzie watersheds show small increases relative to GRACE and annual runoff. With longer time series, the uncertainties would be reduced by way of the $1/\sqrt{N}$ factor where N is the number of series data. This suggests the differences of the secular magnitudes of the GRACE water equivalent mass change to those of annual runoff are due to a component of water equivalent mass change. The values are +5.34 km^3/yr (b_1, Lena), +23.11 km^3/yr (b_2, Yenisei), +0.98 km^3/yr (b_3, Ob') and -5.54 km^3/yr (b_4, Mackenzie).

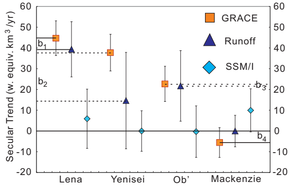

Figure 5. Comparison of secular trend magnitudes and uncertainties.

Continuous permafrost, as a percentage of the total watershed area varies from about 80% in Lena, 32% in Yenisei, 1% in Ob', and 30% in Mackenzie (*Serreze et al.*, 2003). Given that continuous permafrost acts as an aquaclude whereas talik (unfrozen material within permafrost) acts as an aquifer, we hypothesize that the differences (Fig. 5) are linked to the development of open- and closed-talik, within the continuous zone and the decrease of permafrost in the discontinuous zone. Talik in continuous permafrost can form pathways for groundwater, connecting sub-, inter- and suprapermafrost groundwater to lakes and river channels (Woo, 1993; *Yoshikawa et al.*, 2006). Long-term expansion of existing taliks and new open-taliks at depth can be driven by thermokarst processes associated with river migration and lake expansion (*Crampton*, 1979; *Yoshikawa and Hinzeman*, 2003; *Shuur et al.*, 2008). Open-talik development and expansion could have the potential of reducing groundwater residence-time by storage depletion and conversely increase groundwater residence-time by recruitment of surface water into groundwater storage. These considerations indicate eq. (1) can be evaluated as

$$\Delta G \cong \Delta T_{GRACE} - \Delta R$$

in the Arctic permafrost watersheds of Eurasia and North America. Therefore, the biases of the secular magnitudes of the GRACE trends with those of annual runoff trends point to three deductions:

1.Lena and Yenisei increased in groundwater storage.
2.Ob' had no change in groundwater storage.
3.Mackenzie decreased in groundwater storage.

Conclusion

In this study we have shown comparisons of the low degree-order GRACE water equivalent mass changes with SSM/I SWE, and AMSR-E VWC and SMC, and monthly in-situ runoff on the Eurasian and North American Arctic watersheds. Results indicated that the GRACE secular trends captured changes of ground water storage of the continuous permafrost within the watersheds. We hypothesize that these changes are linked to expansions of existing open-taliks, and development of new through-taliks..

Acknowledgements

R.R. Muskett was funded by grants through Dr. V.E. Romanovsky from the National Science Foundation. The Japan Aerospace Exploration Agency is thanked for use of their cluster computing facilities at the International Arctic Research Center. The Alaska Region Supercomputing Center is thanked for providing computing facilities support. GRACE data were processed by Dr. D.P. Chambers, supported by the NASA Earth Science REASoN GRACE Project (http://grace.jpl.nasa.gov). R.R. Muskett performed this work at the International Arctic Research Center, Univ.ersity of Alaska Fairbanks, AK, USA.

References

Chambers, D.(2006), Observing seasonal steric sea level variations with GRACE and satellite altimetry, *J. Geophys. Res.*, 111, C03010, doi: 10.1029/2005JC002914.
Chang, A.T.C., J.L. Foster, and D.K. Hall (1987), Nimbus-7 SMMR derived global snow cover parameters, Annals of Glaciol., 9, 39-44.
Crampton, C.B. (1979), Changes in permafrost distribution produced by a migrating river meander in the northern Yukon, Canada, Arctic, 32 (2), 148-151.
Frappart, F., G. Ramillien, S. Biancamaria, N.M. Mognard, and A. Cazenave (2006), Evolution of high-latitude snow mass derived from the GRACE gravimetry mission (2002-2004), Geophys. Res. Lett., 33, L02501,doi: 10.1029/2005GL024778.
Mudelsee, M., M. Börngen, G. Tetzlaff, and U. Grünewald (2003), No upward trends in the occurrence of extreme floods in central Europe, Nature, 425, 116-169.
Niu, G.-Y., K.-W. Seo, Z.-L. Yang, C. Wilson, H. Su, J. Chen, and M. Rodell (2007), Retrieving snow mass from GRACE terrestrial water storage change with a land surface model, Geophys. Res. Lett., 34, L15704, doi: 10.1029/2007GL03413.
Osterkamp, T.E. (2007), Charasteristics of the recent warming of permafrost in Alaska, *J. Geophys. Res.*, 112, F02S02, doi: 10.1029/2006JF000578.
Paulson, A., S. Zhong, and J. Wahr (2007), Inference of mantle viscosity from GRACE and relative sea level data, *Geophys. J. Int.*, 171: 497-508, doi: 10.1111/j.1365.246X.2007.03556.x.
Ramillien, G., S. Bouhours, A. Lombard, A. Cazenave, F. Flechtner, and R. Schmidt (2008), Land water storage contributions to sea level from GRACE geoid data over 2003-2006, Global & Planet. Change, 60, 381-392,doi: 10.1016/j.gloplacha.2007.04.002.
Romanovskii, N.N., H.W. Hubberten, A.V. Gavrilov, V.E. Tumskoy, G.S. Tipenko, M.N. Grigoriev, and C. Siegert (2000), Thermokarst and Land-Ocean Interaction, Leptev Sea Region, Perma. and Perigl. Processes, 11, 137-152.
Romanovsky, V.E., T.S. Sazonova, V.T. Balohaev, N.I. Shender, and D.O.Sergueev (2007), Past and recent changes in air and permafrost temperaturesin eastern Siberia, *Global & Planet. Change*, 56, 399-413,doi: 10.1016/j.gloplacha.2006.07.023.
Serreze, M.C., D.H. Bromwich, M.P. Clark, A.J. Etringer, T. Zhang, and R. Lammers (2003), Large-scale hydor-climatology of the terrestrial Arctic drainage system, J. Geophys. Res., 108 (D2), 8160, doi:10.1029/2001JD000919.
Shuur, E.A.G., J. Bockeim, J.G. Canadell, E. Euskirchen, C.B. Field, S.V. Goryachkin, S. Hagemann, P. Kuhry, P.M. Lafleur, H. Lee, G. Mazhitova, F.E. Nelson, A. Rinke, V.E. Romanovsky, N. Shiklomanov, C. Tarnocai, S. Venevsky, J.G. Vogel, and S.A. Zimov (2008), Vulnerability of permafrost carbon to climate change: Implications for global carbon cycle, Biogeosci., 58 (8), 701-714, doi:10.1641/B580807.
Svendsen, J.I., H. Alexanderson, V.I. Astakhov, I. Demidov, J.A. Dowdeswell, S. Funder, V. Gataullin, M. Henriksen, C. Hjort, M. Houmark-Nielsen, H.W. Hubberten, Ó. Ingólfsson, M. Jakobsson, K.H. Kjær, E. Larsen, H. Lokrantz, J.P. Lunkka, A. Lysa, J. Mangerud, A. Matiouchkov, A. Murray, P. Möller, F. Niessen, O. Nikolskaya, L. Polyak, M. Saarnisto, C. Siegert, M.J. Siegert, R.F. Spielhagen, R. Stein (2004), Late Quaternary ice sheet history of northern Eurasia, Quatern. Sci. Rev., 23, 1229-1271, doi:10.1016/j.quascirev.2003.12.008.
Syed, T.H., J.S. Famiglietti, V. Zlotnicki, and M. Rodell (2007), Contemporary estimates of Pan-Arctic Freshwater discharge from GRACE and reanalysis, Geophys. Res. Lett., 34, L19404, doi: 10.1029/2007GL031254..
White, D., L. Hinzman, L. Alessa, J. Cassano, M. Chambers, K. Falkner, J. Francis, W. J. Gutowski Jr, M. Holland, R. Max Holmes, H. Huntington, D. Kane, M. A. Kliskey, C. Lee, J. McClelland, B. Peterson, T. Scott Rupp, F. Straneo, M. Steele, R. Woodgate, D. Yang, K. Yoshikawa, and T. Zhang (2007), The arctic freshwater system: Changes and impacts, *J. Geophys. Res.*, 112, G04S54, doi: 10.1029/2006JG000353.
Woo, M.-K. (1993), Northern Hydrology, in, Canada's Cold Environments, H.M. French and O. Slaymarker [eds.], 117-142, Montreal and Kingston: McGill-Queen's Univ. Press.
Yang, D., D.L. Kane, L.D. Hinzman, X. Zhang, T., Zhang, and H. Ye (2002), Siberian Lena River hydrologic regime and recent changes, J. Geophys. Res., 107 (D23), 4694, doi: 10.1029/2002JD002542.
Yang, D.Q., B.S. Ye, and A. Shiklomanov (2004), Stream flow changes over Siberian Yenisei River Basin, J. Hydrol., 296 (1-4), 59-80.
Yoshikawa, K. and L.D. Hinzeman (2003), Shrinking thermokarst ponds and groundwater dynamics in discontinuous permafrost near council, Alaska, Perma. and Perigl. Processes, 14, 151-160.
Yoshikawa, K., V. Romanovsky, L. Hinzman, M. Zheleznyak, N. Romanovsky, and S. Buldovich (2006), Intra-permafrost water and hydrological chronology; a case study of aufeis and spring hydrology in continuous permafrost regions, EOS Trans. Am. Geophys. Union, Fall Meeting Supl., U31B-07.
Zhang, T., R.G. Berry, R.G. Knowles, J.A. Heginbottom, J. Brown (1999), Statistics and characteristics of permafrost and ground-ice distribution in the Northern Hemisphere, Polar Geograph., 23, 132-154

Submitted to Environmental Research Letters, April 7, 2009.